"Ultracold Fusion" – Designing Transport Modes for Collision-based Fusion of Ultracold Atomic Nuclei

Brian Dellabetta*

(Dated: August 23, 2025)

Nuclear fusion power concepts based on the collision of individual pairs of atoms are an appealing alternative to the extreme temperatures and pressures that currently hinder thermonuclear fusion reactors from scaling as a sustainable source of energy. Collision-based schemes and applications appear in the literature as far back as the 1970s, but progress stalled because of fundamental issues largely stemming from the parabolic dispersion relation of massive atoms in free space – significant energy is expended to accelerate atoms to a critical velocity, which in turn decreases the de Broglie wavelength and probability of quantum tunneling through the Coulomb barrier. Since those initial investigations, significant progress in ultracold atom technology has shown that carefully designed optical lattices can yield atomic transport modes following a fundamentally different *linear* dispersion relation along certain topological phase transitions – zero effective mass, high velocity, and long wavelength at low energy. Moreover, these modes are confined to one dimension, cannot decelerate or backscatter, and are energetically separated from bulk scattering states. In this perspective, we propose that this emerging technology is the ideal environment to revive the study of practical nuclear fusion reactors based on the collision of individual pairs of atoms, with the promise of being more modular and sustainable than any of the leading thermonuclear fusion candidates.

I. INTRODUCTION

Nuclear fusion reactors have been a topic of immense interest for decades – a viable nuclear fusion reactor could provide immense amounts of clean energy to help resolve long-standing concerns of climate change caused by fossil fuels and increasing global energy demand.

Virtually every current initiative to achieve practical nuclear fusion belongs to the class of thermodynamic nuclear fusion (e.g. magnetic and inertial confinement fusion concepts). A bulk fuel source is confined to an environment of immense temperature and pressure to force atomic nuclei close enough to overcome Coulomb repulsion, fusing them into heavier nuclei and releasing energy. Creating such an environment is an extremely difficult engineering challenge, and it is an open question whether a net positive energy can ever sustainably be harvested from a thermodynamic fusion reactor.

An environment of immense temperature and pressure is not mandatory for nuclear fusion, which is inherently a microscopic reaction between two atomic nuclei, to occur. One alternative, dating back at least to the 1970s, is to collide two beams of atomic nuclei at a high enough velocity to overcome Coulomb repulsion and trigger fusion, known as Colliding Beam Fusion (CBF) [1–3].

The most naive CBF design is shown in Fig. 1a. While CBF appears in the literature spanning multiple decades, it failed to ever produce a net positive energy (see Appendix A for a brief review). The fatal flaw ultimately lies in the parabolic dispersion relation of massive atoms in free space (see Table I). First and foremost, significant energy ($\sim$ 100 keV per atom pair) is needed to accelerate atoms to a sufficient velocity, meaning CBF has a high variable energy cost. For massive particles, high energy will result in a short de Broglie wavelength ($E \propto 1/\lambda$), which will decrease so-called "geometric factor" of the fusion cross section, $\sigma \propto \lambda_{dB}^2$ [4]. Furthermore, the energy lost to screening and scattering effects into a continuum of lower-energy states, known as bremsstrahlung loss, is prohibitively large to ever yield a net positive energy [5]. For these reasons, CBF research appears to have stalled in the 1990s.

* Correspondence: brian.dellabetta@gmail.com

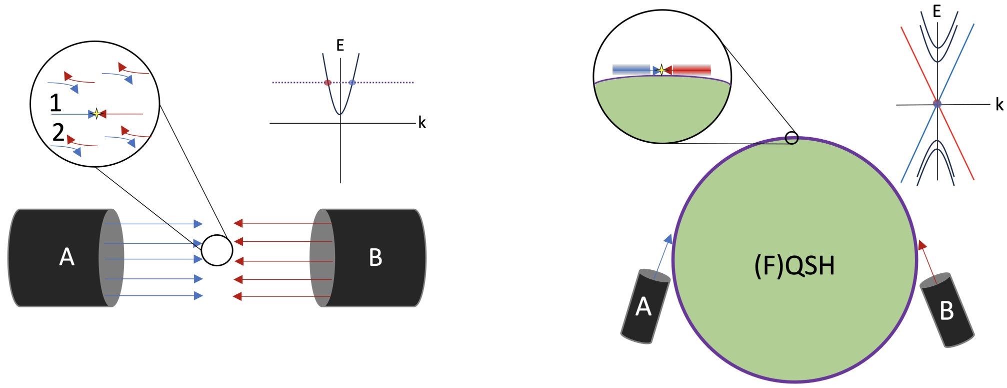

(a) (b)

FIG. 1: a) In the most naive approach for CBF, fusible atoms A (blue) and B (red) collide with one another at sufficient velocity to trigger fusion (inset #1), but too much energy is lost to scattering and screening effects to achieve a net positive (inset #2). *Top-right*: parabolic dispersion relation for massive particles in a vacuum, indicating the amount of energy needed to reach critical velocity (purple dashed line). b) Proposal for collision-based fusion of ultracold atoms along the topologically nontrivial (Floquet) Quantum Spin Hall state. Two 1-D edge modes (purple) reside along the phase transition between the topologically nontrivial (green) and trivial (white) regions. Fusible atoms A and B in these edge modes are exponentially pinned to the surface (inset, shaded blue and red). *Top-right*: idealized linear dispersion relation for the Floquet Quantum Spin Hall state, where topological edges modes (red and blue lines) are energetically separated from bulk states (black lines). The location of the band crossing is dictated by the topological phase and optical lattice, though ideally would cross at vanishing energy and wave number.

II. NEW PERSPECTIVE

In free space, high-velocity atoms will have a high energy and a short wavelength. Qualitatively different dispersion is necessary for CBF to be viable – high-speed, low energy, and long wavelength (i.e. nuclei are wave-like rather than point-like, so that the wave functions of their nuclei overlap). Condensed matter physics has shown charged particles can have fundamentally different behavior in a periodic potential vs. free space (see Appendix B for a brief review). Indeed, modes exhibiting the desired dispersion relation have been shown to exist along the boundary of certain topological phase transitions. Namely, a signature of the Quantum Spin Hall (QSH) topological phase is a pair of counterpropagating, high-speed, one-dimensional modes along the phase transition.

Optical lattices (i.e. lattices created from laser light) are an emerging technology for the control and manipulation of ultracold atomic nuclei (see Appendix C for a brief review). What holds for electrons in a crystalline atomic lattice has also been shown to hold for atomic nuclei in optical lattices. Topological phases have been experimentally realized in optical lattices, and several proposals exist for the desired QSH phase.

The proposed "Ultracold Fusion" design is depicted in Fig. 1b – cool and place atomic nuclei in the counter-propagating, high-speed, high-wavelength modes that appear along the boundary of an optical lattice in a QSH topological phase. The key enhancements in the proposed form are the following:

1. Ultracold atoms following a linear dispersion are much more likely to quantum tunnel than atoms following parabolic dispersion in free space. In the semiclassical picture, the quantum tunneling probability of massive particle decays exponentially with respect to initial energy,

	CBF (1970s)	Ultracold Fusion Proposal
Hamiltonian Kinetic Operator	$\hat{T} = \frac{-\hbar^2}{2m}\frac{\partial^2 \Psi}{\partial x^2}$	$\hat{T} = -i\hbar v_F \frac{\partial \Psi}{\partial x}$
Semiclassical Tunneling Particle at E_0 into $V(x) = \frac{V_N}{\lvert x \rvert}$ (Appendix D)	$\lvert\Psi(x)\rvert \propto e^{-(V_N - E_0)x}$	constant, independent of E_0
Group Velocity	$v \propto E$	v_F (constant)
Energy Scale	~ 100 keV	$\lll 1$ keV
Wavelength Scale	~ 10 pm	$\ggg 1$ nm

TABLE I: Comparison of critical parameter relationships in conventional CBF vs. ultracold fusion proposal, along with typical magnitudes needed for deuterium-tritium fusion.

whereas quantum tunneling rate of massless particles is *constant*, independent of initial energy (see Appendix D for derivation).

2. The variable cost of accelerating atomic nuclei to a critical velocity in free space is converted to a fixed cost of operating the optical lattice, so a low fusion rate need not be a deal-breaker for positive energy yield. The one-dimensional modes are periodic, so atoms will cycle indefinitely until scattering into bulk states.

3. Wavelength of topological edge modes can be designed to be at least a few orders of magnitude higher than picometer-scale (10^{-12} m) wavelengths typical of CBF, resulting in an enhancement of several orders of magnitude on the geometric factor of the fusion cross section, $\sigma \propto \lambda_{dB}^2$ [4].

4. Atoms in free space have a continuum of scattering states in which to decelerate or change trajectory. Ultracold atoms in topological edge modes are protected from backscattering and are energetically separated from bulk bands [6]. The loss of bremsstrahlung should effectively be zero in the ideal band structure shown in Fig. 1b, and while scattering in bulk states is still possible, at least no energy will be lost to it.

5. Atoms should be much more concentrated in the transverse direction, significantly increasing the probability of collision. In CBF, the beam cross sections are on the order of 1000 cm^2 [3] (although this is likely much lower with current technology), following a $1/r^2$ relationship [3] that disperses outward from the aperture. In the proposed design, atoms are confined in low-dimensional modes along the phase transition, following a e^{-r^2} relationship that does not disperse provided it does not scatter into a bulk state (see Appendix B for more details).

III. CONCLUSION & OPEN QUESTIONS

The design of transport modes most suitable for fusion of ultracold atomic nuclei offers a promising playground to revisit CBF, and potentially circumvent the extreme environments necessary for thermodynamic fusion reactors. Optical lattices provide flexible control over the salient features for fusion – effective mass, edge mode velocity, spatial confinement in the transverse directions, and band gap energy separation from bulk states.

Ultimately, the viability of ultracold fusion will depend on estimating fusion and scattering rates as functions of edge mode velocity and bulk band gap separation, beyond the semiclassical picture (see Appendix E for an initial attempt). As an upper bound, modern laser technology is capable of achieving QSH optical lattices with the same velocity as used in CBF, but would require sub-nm laser wavelengths and approaches the limits of feasibility (see Appendix C 1 for detail). Here, we simply hope to have motivated a promising general framework meriting further exploration, concluding with some open questions:

1. *How does broken spin-rotation symmetry affect the result?* Atoms in the edge modes are spin-momentum locked, i.e. atoms moving clockwise all have the same spin, which is opposite the spin of atoms moving counter-clockwise). Would this have an effect on the scattering trajectory of the resultant high-energy output particles? Practical applications aside, this appears to be a promising environment for probing some unique physics.

2. *What happens if fusion does occur?* The resultant high-energy (14 MeV) neutron as a charge-free particle would not be bound to the edge mode. Its energy could presumably be captured as heat in a heavy water reservoir. The resultant charged particle would have energy on the order of MeV, far exceeding the band gap, and could be captured easily. Could it inadvertently damage the optical lattice or FQSH state?

3. *What happens if fusion does not occur?* Edge modes atoms would either pass by one another or scatter into bulk states. Even if there is only a low probability that two counter-propagating atoms fuse, if the lifetime of an edge mode atomic state is long, it could feasibly pass by many counter-propagating atoms, increasing the number of chances it has to fuse provided scattering rates are low and atoms in edge mode states have long lifetimes.

---

[1] B. C. Maglich, The migma principle of controlled fusion, Nuclear Instruments and Methods **111**, 213 (1973).

[2] B. Maglich, M. Mazarakis, R. A. Miller, J. Nering, S. Channon, and C. Powell, Self collliding beams ("migma") and controlled fusion, IEEE Transactions on Nuclear Science **NS-22**, 1790 (1975).

[3] J. P. Blewett, Fusion reactions in colliding beams, (197x).

[4] X. Z. Li, B. Liu, Q. M. Wei, S. X. Zheng, and D. X. Cao, Fusion cross sections for fusion energy, Fusion Engineering and Design **81**, 1517 (2006), proceedings of the Seventh International Symposium on Fusion Nuclear Technology.

[5] T. H. Ridder, A general critique of inertial-electrostatic confinement fusion systems, Phys. Plasmas **2**, 1853 (1995).

[6] X.-L. Qi and S.-C. Zhang, Topological insulators and superconductors, Rev. Mod. Phys. **83**, 1057 (2011).

[7] A. Cheung, M. Binderbauer, F. Liu, A. Qerushi, N. Rostoker, and F. Wessel, Colliding beam fusion reactor space propulsion system, (2004).

[8] N. Rostoker and A. Qerushi, Equilibrium of field reversed configurations with rotation. i. one space dimension and one type of ion, Physics of Plasmas **9**, 3057 (2002), https://doi.org/10.1063/1.1475683.

[9] X.-G. Wen, Topological order: From long-range entangled quantum matter to a unified origin of light and electrons, ISRN Condensed Matter Physics **2013**, 1 (2013).

[10] M. Fruchart and D. Carpentier, An introduction to topological insulators, Comptes Rendus Physique **14**, 779 (2013), topological insulators / Isolants topologiques.

[11] C. L. Kane and E. J. Mele, Z_2 topological order and the quantum spin hall effect, Phys. Rev. Lett. **95**, 146802 (2005).

[12] C. L. Kane and E. J. Mele, Quantum spin hall effect in graphene, Phys. Rev. Lett. **95**, 226801 (2005).

[13] B. A. Bernevig, T. L. Hughes, and S.-C. Zhang, Quantum spin hall effect and topological phase transition in hgte quantum wells, Science **314**, 1757 (2006), https://www.science.org/doi/pdf/10.1126/science.1133734.

[14] M. König, S. Wiedmann, C. Brüne, A. Roth, H. Buhmann, L. W. Molenkamp, X.-L. Qi, and S.-C. Zhang, Quantum spin hall insulator state in hgte quantum wells, Science **318**, 766 (2007), https://www.science.org/doi/pdf/10.1126/science.1148047.
[15] I. Bloch, J. Dalibard, and W. Zwerger, Many-body physics with ultracold gases, Rev. Mod. Phys. **80**, 885 (2008).
[16] J. Nemirovsky and Y. Sagi, Fast universal two-qubit gate for neutral fermionic atoms in optical tweezers, Phys. Rev. Res. **3**, 013113 (2021).
[17] L. Tarruell and L. Sanchez-Palencia, Quantum simulation of the hubbard model with ultracold fermions in optical lattices, Comptes Rendus Physique **19**, 365 (2018), quantum simulation / Simulation quantique.
[18] F. Schäfer, T. Fukuhara, S. Sugawa, Y. Takasu, and Y. Takahashi, Tools for quantum simulation with ultracold atoms in optical lattices, Nature Reviews Physics **2**, 411 (2020).
[19] L. Amico, M. Boshier, G. Birkl, A. Minguzzi, C. Miniatura, L.-C. Kwek, D. Aghamalyan, V. Ahufinger, D. Anderson, N. Andrei, A. S. Arnold, M. Baker, T. A. Bell, T. Bland, J. P. Brantut, D. Cassettari, W. J. Chetcuti, F. Chevy, R. Citro, S. D. Palo, R. Dumke, M. Edwards, R. Folman, J. Fortagh, S. A. Gardiner, B. M. Garraway, G. Gauthier, A. Günther, T. Haug, C. Hufnagel, M. Keil, P. Ireland, M. Lebrat, W. Li, L. Longchambon, J. Mompart, O. Morsch, P. Naldesi, T. W. Neely, M. Olshanii, E. Orignac, S. Pandey, A. Pé rez-Obiol, H. Perrin, L. Piroli, J. Polo, A. L. Pritchard, N. P. Proukakis, C. Rylands, H. Rubinsztein-Dunlop, F. Scazza, S. Stringari, F. Tosto, A. Trombettoni, N. Victorin, W. von Klitzing, D. Wilkowski, K. Xhani, and A. Yakimenko, Roadmap on atomtronics: State of the art and perspective, AVS Quantum Science **3**, 039201 (2021).
[20] D.-W. Zhang, Y.-Q. Zhu, Y. X. Zhao, H. Yan, and S.-L. Zhu, Topological quantum matter with cold atoms, Advances in Physics **67**, 253 (2018).
[21] K. Wintersperger, C. Braun, F. N. Ünal, A. Eckardt, M. D. Liberto, N. Goldman, I. Bloch, and M. Aidelsburger, Realization of an anomalous floquet topological system with ultracold atoms, Nature Physics **16**, 1058 (2020).
[22] C. Braun, R. Saint-Jalm, A. Hesse, J. Arceri, I. Bloch, and M. Aidelsburger, Real-space detection and manipulation of topological edge modes with ultracold atoms (2023), arXiv:2304.01980 [cond-mat.quant-gas].
[23] C. J. Kennedy, G. A. Siviloglou, H. Miyake, W. C. Burton, and W. Ketterle, Spin-orbit coupling and quantum spin hall effect for neutral atoms without spin flips, Phys. Rev. Lett. **111**, 225301 (2013).
[24] G. Liu, S.-L. Zhu, S. Jiang, F. Sun, and W. M. Liu, Simulating and detecting the quantum spin hall effect in the kagome optical lattice, Phys. Rev. A **82**, 053605 (2010).
[25] D. Cocks, P. P. Orth, S. Rachel, M. Buchhold, K. Le Hur, and W. Hofstetter, Time-reversal-invariant hofstadter-hubbard model with ultracold fermions, Phys. Rev. Lett. **109**, 205303 (2012).
[26] N. Goldman, I. Satija, P. Nikolic, A. Bermudez, M. A. Martin-Delgado, M. Lewenstein, and I. B. Spielman, Realistic time-reversal invariant topological insulators with neutral atoms, Phys. Rev. Lett. **105**, 255302 (2010).
[27] Z. Yan, B. Li, X. Yang, and S. Wan, A general time-periodic driving approach to realize topological phases in cold atomic systems, Scientific Reports **5**, 16197 (2015).
[28] N. Goldman, J. Dalibard, A. Dauphin, F. Gerbier, M. Lewenstein, P. Zoller, and I. B. Spielman, Direct imaging of topological edge states in cold-atom systems, Proceedings of the National Academy of Sciences **110**, 6736 (2013), https://www.pnas.org/doi/pdf/10.1073/pnas.1300170110.
[29] M. Aidelsburger, personal communication.
[30] H. Yoneda, Y. Inubushi, K. Nagamine, Y. Michine, H. Ohashi, H. Yumoto, K. Yamauchi, H. Mimura, H. Kitamura, T. Katayama, T. Ishikawa, and M. Yabashi, Atomic inner-shell laser at 1.5-ångström wavelength pumped by an x-ray free-electron laser, Nature **524**, 446 (2015).
[31] N. Thomson, L. Moschini, and A. Diaz-Torres, Laser-assisted deuterium-tritium fusion: A quantum dynamical model, Phys. Rev. C **110**, 034614 (2024).
[32] S. Liu, H. Duan, D. Ye, and J. Liu, Deuterium-tritium fusion process in strong laser fields: Semiclassical simulation, Physical Review C **104**, 10.1103/physrevc.104.044614 (2021).
[33] J. J. Bekx, M. L. Lindsey, S. H. Glenzer, and K.-G. Schlesinger, Applicability of semiclassical methods for modeling laser-enhanced fusion rates in a realistic setting, Phys. Rev. C **105**, 054001 (2022).
[34] M. Fowler, *Quantum Mechanics*, Chap. 8.2: The WKB Approximation.
[35] R. G. Littlejohn, Green's functions in quantum mechanics, (2020).

Appendices

A. COLLIDING BEAM FUSION

CBF dates back to at least 1973 [1]. CBF has been proposed for a wide range of output-power levels (MWs to GWs) and fuels, such as D-D, D-T, D-He^3, H-$B^1$1, and H-Li^6 (D and T here denote deuterium and tritium) [7, 8]. To highlight the fatal flaw of CBF, we summarize the most naive approach for a D-T fusion reaction:

$$\text{deuteron} + \text{triton} \rightarrow \alpha + \text{neutron} \tag{1}$$

All numbers are pulled from ref. [3]. At 100 keV, i.e. when the atoms differ in velocity by 3×10^6m/s, the reaction cross section has a max of $\sigma_f \approx 5$ barns (see Fig. 1 of Maglich et al. [2] for a more comprehensive chart of fusion cross section vs. beam energy). Of the 17 MeV of energy produced on the right hand side, 14 MeV resides on the neutron as kinetic energy. Given a beam width cross section of 1000 cm^2 and D/T atom concentrations of 6×10^{18} m^{-3}, ref. [3] estimates a fusion yield of 0.65 W per meter of distance along the colliding beams, an extremely poor yield given 60 MW have gone into producing the two colliding beams. Although this naive setup can be improved with magnetic confinement or by recycling the ions in a cylindrical setting to allow multiple opportunities to fuse, the fusion cross section is simply too small relative to the spatial confinement of the beams to ever be viable. Screening and scattering effects further degrade the fidelity of the beams.

B. TOPOLOGICAL ORDER IN CONDENSED MATTER

There is a rich history of the study of topological order in condensed matter systems dating back to the late 1980s [9]. We focus on Topological Insulators, a relatively new state of quantum matter characterized by a full insulating gap and a nontrivial topological order parameter we denote $m < 0$ [6]. The existence of topological order in an insulator exhibits unique behavior, the most universal and remarkable one (and the most important for us) being the existence of gapless edge or surface states at the boundary with a state of trivial topological order $m > 0$ (i.e. at the phase transition) [10].

We are concerned with one-dimensional helical edge modes, i.e. two counter-propagating edge modes of opposite spin. A 2D topological insulator, also known as a Quantum Spin Hall (QSH) insulator, is shown with edge modes and dispersion in Fig. 2a. The theory, prediction, and experimental realization of the QSH effect date to the mid 2000s [11–14]. The electronic edge mode wave function is (see Section 3.5.7 of [10] for a nice derivation):

$$\psi(x, y) \propto e^{iq_x x} \exp\left[-\int_0^y m(y')dy'\right] \begin{bmatrix} 1 \\ \\ 1 \end{bmatrix}, \tag{2}$$

where x and y are the longitudinal and transverse directions, respectively. This means the spatial confinement of the helical edge modes at the phase transition is exponentially pinned by the magnitude of the topological order parameter $m(y)$, as shown in Fig. 2b.

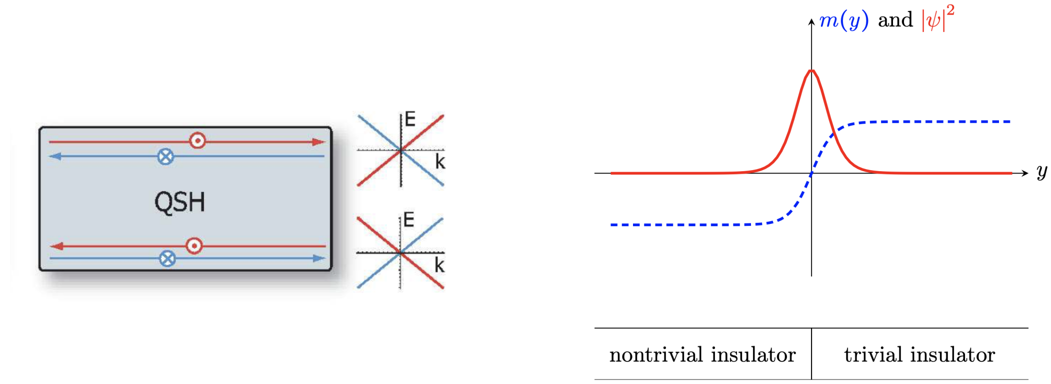

(a) (b)

FIG. 2: a) Counter-propagating edge modes of opposite spin and linear dispersion are a signature of the Quantum Spin Hall state. Image from [6]. Red denotes spin-up, blue denotes spin-down. The modes are gapless, yielding quasiparticles with zero effective mass. b) The edge state wave function is exponentially pinned at the phase transition where mass gap $m(y)$ goes from negative to positive. Image from [10].

Two additional traits, not found in CBF, are critical. First, these edge modes are protected from backscattering by time-reversal symmetry; all possible backscattering paths destructively interfere as long as impurities are nonmagnetic [6]. Second, edge modes have linear dispersion – electronic quasiparticles are effectively massless and have high velocity (which is proportional to the slope of the dispersion, $v \propto \frac{\partial E}{\partial k}$) even at low energy. In CBF, a significant amount of energy was needed to create beams with high enough velocity to overcome the Coulomb barrier, much of which was then lost to scattering and screening effects. The same velocity can be realized for low- or zero-energy quasiparticles in these edge states.

C. ULTRACOLD ATOMS AND ATOMTRONICS

Ultracold atom systems use laser cooling and magneto-optic traps to spatially confine and manipulate atoms at temperatures close to absolute zero. These systems allow for a remarkable deal of flexibility and control, from experimental realization of exotic states like Bose-Einstein condensates [15] to applications in quantum computing [16]. Additionally, they provide a platform for creating and simulating in an optical lattice a variety of models initially introduced in condensed matter physics [17, 18]. This has simultaneously paved the way for another field coined ”atomtronics” [19], which deals with the engineered manipulation of ultracold atoms, through magnetic or laser-generated guides, to create atomic components analogous to electronic components, e.g. diodes and transistors.

Topological phases in cold atom systems have been realized for a number of toy models originally proposed in condensed matter physics [20, 21]. More recently, Braun et al. [22] create a topological phase in a 2D Floquet system (i.e. with time periodic hopping), driving the system from a topologically trivial to non-trivial state with a periodic optical potential that preserves time-reversal symmetry and observing signatures of topological phase changes with with real-space measurements of the edge current.

Although these are chiral currents in a single direction and no published experimental realization of the QSH effect in cold atom systems has been reported to our knowledge, several papers propose schemes for creating it [23–27] and observing it [28] with similar Floquet dynamics. As a point of emphasis, Zhang et al. [27] comment ”the edge states are helical in the sense that fermionic atoms with opposite spin propagate in opposite direction”. According to the PI of [22], this amounts to tuning to a different region of the phase diagram, and in principle there is no particular reason why this in principle should not be possible [29].

1. *Achieving Critical Velocity*

The FQSH state thus provides the necessary qualities outlined above, with many degrees of freedom for finding the optimal configuration. Note the band structure diagram in Fig. 1b can be (1) stretched in the vertical direction by scaling every energy and frequency in the optical lattice Hamiltonian by the same factor, or (2) squeezed in the horizontal direction by scaling down the optical lattice constant. Edge mode velocity, bulk band gap, and spatial confinement are all implicitly tuneable. We conclude this section by considering the system requirements to achieve fusible edge mode velocities.

Braun et al. [22] report velocities on the order of mm/s with a laser wavelength $\lambda_L = 745$ nm, hexagonal optical lattice spacing of $a = 287$ nm, and Floquet frequencies in the kHz regime. This is rouhgly 9 orders of magnitude below the critical velocities on the order of 10^6 m/s discussed in Appendix A. Fortunately, edge mode velocity scales very favorably with respect to optical lattice laser wavelength λ_L. Hopping energies are set by the Floquet frequencies and the recoil energy [18],

$$E_r = \frac{\hbar^2 k_L^2}{2M} \propto \frac{1}{\lambda_L^2}, \tag{3}$$

and the lattice constant scales directly with laser wavelength, $a \propto \lambda_L$. Edge mode velocity with linear dispersion will thus scale

$$v \propto \frac{1}{\lambda_L^3}, \tag{4}$$

two orders of magnitude coming from the energy scaling and one order of magnitude coming from the lattice constant scaling.

Critical velocities on the order of 10^6 m/s should not be necessary in topological bands, however we will use it as an absolute upper bound for lack of a better answer. Velocity would have to increase by roughly 9 orders of magnitude from mm/s, which would necessitate an optical lattice laser wavelength roughly 3 orders of magnitude smaller accompanied by a scaling of all hopping energies and Floquet frequencies by 6 orders of magnitude. This would require 0.75 nm wavelength optical lattices and Floquet frequencies in the GHz regime. The current world record for shortest laser wavelength is 0.15 nm [30], though such an energy scaling could very well introduce unwanted higher-order / non-linear effects that degrade the system or introduce other hurdles. We reiterate though that this would be an upper bound on critical velocity, sub-nm wavelength lasers are likely not necessary. This estimation remains as the key open question.

D. SEMICLASSICAL APPROXIMATION OF QUANTUM TUNNELING

This section will solve the one-dimensional time-independent Schrodinger equation in the semiclassical picture to emphasize the qualitatively different quantum tunneling behavior between linear and parabolic dispersion. We will consider a free particle at energy E_0 moving rightwards toward another particle at rest at $x = 0$, so that the Coulomb potential is $V(x) = \frac{V_N}{|x|}$ where $V_N \gg E_0$.

We will study this in the semiclassical limit, i.e. when $V(x)$ is slowly varying with respect to the wavelength of the incident particle. *(Note: it is not clear if the slowly varying potential assumption is valid if V(x) can vary significantly at the fm* (10^{-15}) *scale but wavelengths are on the order of pm* (10^{-12}) *or nm. Nonetheless it is commonly used in theoretical models for nuclear fusion [31–33]).*

1. *Free Space, Parabolic Dispersion*

We first present the results for a massive particle in free space, a common exercise in a quantum mechanics course [34] (full derivation available here). The wavefunction $\psi(x)$ can be determined by solving the the time independent Schrodinger equation,

$$-\frac{\hbar^2}{2m}\frac{d^2\psi(x)}{dx^2} + V(x)\psi(x) = E\psi(x). \tag{5}$$

In the semiclassical limit, the wave function can be written in the form

$$\psi(x) = e^{(i/\hbar)p(x)}. \tag{6}$$

where $p(x)$ denotes the localized momentum defined classically by

$$p^2(x)/2m + V(x) = E. \tag{7}$$

The solution to this problem, to leading order, is widely known as the WKB approximation,

$$\begin{aligned}\psi(x) &= \exp\big[\frac{i}{\hbar}\int\sqrt{2m(E-V(x))}dx\big]\\ &= \exp\big[\frac{-1}{\hbar}\int\sqrt{(2m(V_N-E_0)/x)}dx\big].\end{aligned} \tag{8}$$

Quantum tunneling probability thus decays exponentially into the Coulomb barrier:

$$\boxed{\psi(x) \propto e^{(-\sqrt{2m(V_N-E_0)x}/\hbar)}}. \tag{9}$$

A high incident energy is required for massive particles to overcome Coulomb repulsion and achieve fusion.

2. *Topological Edge Mode, Linear Dispersion*

The result in the case of massless particle is simpler to derive, involves no WKB-style approximation, and is much more favorable. Here the time independent Schrodinger equation is

$$-i\hbar v_F\frac{d\psi(x)}{dx} + V(x)\psi(x) = E\psi(x), \tag{10}$$

which, for an incident particle of energy E_0 and a Coulomb potential $V(x) = \frac{V_N}{|x|}$, results in a first-order ODE

$$\frac{d\psi(x)}{dx} = \frac{i(V_N-E_0)}{\hbar v_F}\frac{\psi(x)}{x}. \tag{11}$$

Noting that the solution to $\frac{dy}{dx} = \frac{Ay}{x}$ is $y(x) = c_1x^A$, this yields a quantum tunneling probability,

$$\boxed{\psi(x) = x^{i(V_N - E_0)/(\hbar v_F)}}. \tag{12}$$

that oscillates in x with a frequency that increases as the particle approaches $x = 0$, but **does not decay into the barrier**. $|\psi(x)|^2$ in this case is a constant value independent of incident energy E_0. In the semiclassical limit, atoms counterpropagating along topological edge modes will collide and tunnel with a probability independent of incident energy or velocity. *Is this the right interpretation?*

E. HOW TO MODEL SCATTERING?

This section outlines how scattering might be modeled for two edge mode particles approaching one another, and ultimately depends on how scattering changes with respect to band gap energy and Coulomb repulsion.

Because edge mode particles cannot be back-scattered or decelerated, this may be reducible to a single-state Hamiltonian with decay:

$$\begin{aligned} \mathcal{H} &= V - \frac{i\Gamma}{2} \\ &= \frac{E_0 - V_N}{x_0 - 2v_0 t} - \frac{i\Gamma}{2}, \end{aligned} \tag{13}$$

for a particle in edge mode at energy E_0 and velocity v_0, approaching a counterpropagating edge particle a distance x_0 away at time $t = 0$. The factor of 2 on $v_0 t$ is due to each particle moving towards one another. Γ denotes decay into bulk states due to scattering, and is likely a function of topological band gap energy E_g and potential $V(t)$.

We want to determine the probability the particle is still in the edge mode, and hasn't scattered out, by the time $x_0 - v_0 t$ approaches the femtometer scale necessary for nuclear fusion. This is known as the outgoing, time-dependent Green's function [35]:

$$\langle \psi(t = \frac{v_0}{x_0 - 1\ \mathrm{fm}}) \mid \mathcal{U}(t, t') \mid \psi(t' = 0) \rangle, \tag{14}$$

where $\mathcal{U}(t, t')$ is the time evolution operator from time t' to t.

If Γ is time-independent, the probability of the edge mode scattering before it reaches a distance where fusion can occur, this amounts to a decay rate of $e^{-\Gamma t}$, but doesn't capture how scattering changes when the edge mode particle's potential increases as it approaches the counterpropagating particle. *How should Γ be modified to account for higher scattering rates at higher potential? Does scattering follow a $\Gamma \sim e^{-E_g}$ relation?*